

Advanced Simulation of Quantum Computations: Compact Representation Rather than Hardware Power

Alwin Zulehner *Student Member, IEEE*, and Robert Wille *Senior Member, IEEE*

Abstract—Quantum computation is a promising emerging technology which, compared to classical computation, allows for substantial speed-ups e.g. for integer factorization or database search. However, since physical realizations of quantum computers are in their infancy, a significant amount of research in this domain still relies on simulations of quantum computations on classical machines. This causes a significant complexity which current state of the art simulators tackle by applying massive hardware power. In this work, we revisit the basics of quantum computation, investigate how corresponding quantum states and quantum operations can be represented, and, eventually, simulated in a more efficient fashion. This leads to a simulation approach which works complementary different to the state-of-the-art. Experimental evaluations show that the proposed solution is capable of simulating quantum computations with more qubits than before, and in significantly less run-time (several magnitudes faster compared to previously proposed simulators). An implementation of the proposed simulator is publicly available online.

I. INTRODUCTION

Quantum computation [12] has become a promising technology which has theoretically been proven to be superior to classical computation for important applications. For example, quantum algorithms for integer factorization (the well-known Shor’s algorithm [17]) or database search (Grover’s Search [6]) have been proposed that lead to significant – sometimes even exponential – speedups compared to classical computations. With respect to physical implementations, significant progress has been made in the recent years as well [8], [16], [4], [11], [10]. Hence, there is an increasing probability that this technology will make it into practice in the near future.

However, thus far, quantum computation remains an emerging technology. This requires, besides others, that respective developments have to be conducted while still relying on classical technologies. In particular, this is an issue when it comes to simulating quantum computations or corresponding quantum algorithms. Although these quantum computations describe approaches to solve several problems significantly faster than a classical technology, they still have to be simulated on classical machines thus far.

This causes a significant obstacle since basic and substantial concepts of quantum computations like superposition, entanglement, or measurement rely on exponentially large vector and matrix descriptions which additionally are composed of complex numbers. Existing methods for the

simulation of quantum computations [5], [21], [18], [7], [9] address this problem using straight-forward methods like simple 1-dimensional and 2-dimensional arrays, respectively. The resulting (exponential) complexity is then tackled by exploiting parallelism and applying massive hardware power such as supercomputers composed of thousands of nodes and more than a petabyte of distributed memory. But even then, quantum systems of rather limited size (today’s practical limit is 46 qubits) can be simulated – additionally often requiring a significant amount of run-time (e.g. up to several days). Current roadmaps show that also future plans rely on the use of massive hardware power, e.g. the authors of [18] expect to simulate 48-49 qubits on a machine with 4-10 petabytes of distributed memory by the year 2020.

In this work, we propose a complementary different approach for the simulation of quantum computations which does not aim to tackle the exponential complexity by pure hardware power, but by an efficient representation. To this end, we revisit the basics of quantum computations and investigate how corresponding simulations can indeed be conducted in a more efficient fashion. These endeavors eventually lead to a significantly more compact representation of quantum states and quantum operations that exploits redundancies in the corresponding description whenever possible. Based on that, a new simulation method is proposed which clearly outperforms the current state-of-the-art.

In fact, the compact representation allows for the simulation of well known quantum algorithms (such as Shor’s Algorithm and Grover’s Search) with more qubits than before – and that on a regular Desktop machine. Finally, with respect to the run-time, a substantial drop can be observed: Instead of several days, the proposed approach is able to complete the simulations within hours – in many cases even just minutes or seconds.

This paper is structured as follows: Section II revisits the basics of quantum computation. In Section III, we investigate the obstacles of simulating quantum computations and review how the current state-of-the-art copes with these issues. Section IV introduces the proposed representation and resulting simulation approach. Finally, the proposed solution is evaluated and compared to the state-of-the-art in Section V, while Section VI concludes the paper.

II. QUANTUM COMPUTATION

Quantum computation significantly differs from the classical computation paradigm. To make this work self-contained and properly introduce our solution, we first briefly revisit the basics on how operations are conducted in this domain. While this ought to be sufficient to comprehend the remainder of this paper, we refer to [12] for a more detailed treatment.

A. Quantum Bits

In classical logic, information is represented by *bits* which can be in one of two basis states 0 and 1. Similarly, quantum computations rely on so called *quantum bits (qubits)* to represent internal states. Again, there exist two basis states, which – using Dirac notation – are denoted $|0\rangle$ and $|1\rangle$. However, in contrast to bits in classical logic, qubits are not restricted to one of these basis states, but may additionally assume an (almost) arbitrary superposition (i.e. a linear combination) of both. More precisely, the state of a qubit is described by $|\psi\rangle = \alpha_0 \cdot |0\rangle + \alpha_1 \cdot |1\rangle$, where the complex factors α_0 and α_1 denote *amplitudes* which indicate how much the qubit is related to the basis states.

The amplitudes of a quantum state $|\psi\rangle$ must satisfy the normalization constraint $|\alpha_0|^2 + |\alpha_1|^2 = 1$. While it is not possible to directly access the values of α_0 and α_1 , it is possible to obtain one of the two basis states by measuring the qubit. More precisely, the basis state $|0\rangle$ is obtained with probability $|\alpha_0|^2$, while $|1\rangle$ is obtained with probability $|\alpha_1|^2$. The measurement collapses (i.e. destroys) the superposition. The concepts discussed above can be generalized for quantum systems composed of multiple qubits. Since each qubit has exactly two basis states, a system composed of n qubits has 2^n basis states – each one represented by $|\{0,1\}^n\rangle$. Overall, this accumulates in the following definition of a quantum state:

Definition 1: Consider a quantum system composed of n qubits. Then, all possible states of the system are of form

$$|\psi\rangle = \sum_{x \in \{0,1\}^n} \alpha_x \cdot |x\rangle, \text{ where } \sum_{x \in \{0,1\}^n} |\alpha_x|^2 = 1 \text{ and } \alpha_x \in \mathbb{C}.$$

The *state* $|\psi\rangle$ can be also represented by a column vector $\psi = [\psi_i]$ with $0 \leq i < 2^n$ and $\psi_i = \alpha_x$, where $\text{nat}(x) = i$.

Note that, to save space, vectors may be provided in their transposed form in the following (indicated by $[\cdot]^T$). That is, the single elements are listed horizontally rather than vertically.

Example 1: Consider a quantum system composed of two qubits which is in the state $|\psi\rangle = \frac{1}{\sqrt{2}}|00\rangle + 0 \cdot |01\rangle + 0 \cdot |10\rangle + \frac{1}{\sqrt{2}}|11\rangle$. This represents a valid state, since $\left(\frac{1}{\sqrt{2}}\right)^2 + 0^2 + 0^2 + \left(\frac{1}{\sqrt{2}}\right)^2 = 1$. The corresponding state vector is

$$\psi = \left[\frac{1}{\sqrt{2}}, 0, 0, \frac{1}{\sqrt{2}} \right]^T.$$

Measuring this system yields one of the two basis states $|00\rangle$ or $|11\rangle$ – both with probability of $|\frac{1}{\sqrt{2}}|^2 = \frac{1}{2}$.

B. Quantum Operations

Quantum operations are used to manipulate the current state of a quantum system. All of them except the measurement are thereby inherently reversible and can be represented by unitary matrices U , i.e. a complex square matrix whose inverse is its conjugate transposed [12]. The size of the matrix depends on the number of involved qubits. Important quantum operations for a single qubit are e.g.

$$X = \begin{bmatrix} 0 & 1 \\ 1 & 0 \end{bmatrix}, \quad H = \frac{1}{\sqrt{2}} \begin{bmatrix} 1 & 1 \\ 1 & -1 \end{bmatrix}, \text{ and } Z = \begin{bmatrix} 1 & 0 \\ 0 & -1 \end{bmatrix},$$

where X complements the current state of the qubit, H sets the qubit into superposition, and Z changes the phase of the qubit, respectively. An important operation involving two qubits is e.g.

$$CNOT = \begin{bmatrix} 1 & 0 & 0 & 0 \\ 0 & 1 & 0 & 0 \\ 0 & 0 & 0 & 1 \\ 0 & 0 & 1 & 0 \end{bmatrix},$$

which performs a so-called controlled inversion.

To evaluate a quantum operation with respect to a given quantum state, the corresponding matrix U has to be multiplied with the corresponding state vector ψ . More precisely:

Definition 2: Consider a quantum system composed of n qubits with

- a quantum operation U represented by a $2^n \times 2^n$ unitary matrix $U = [u_{i,j}]$ with $0 \leq i, j < 2^n$ and
- a system state $|\psi\rangle$ represented by a vector $\psi = [\psi_i]$ with $0 \leq i < 2^n$.

Then, the output state $|\psi'\rangle$ of the quantum system is defined by a vector $\psi' = U \cdot \psi$, i.e. $\psi' = [\psi'_i]$ with

$$\psi'_i = \sum_{k=0}^{2^n-1} u_{i,k} \cdot \psi_k, \quad \text{for } 0 \leq i < 2^n.$$

Example 2: Consider a quantum system composed of two qubits which is currently in state $|\psi\rangle = |11\rangle$. Applying a *CNOT* operation yields

$$\underbrace{\begin{bmatrix} 1 & 0 & 0 & 0 \\ 0 & 1 & 0 & 0 \\ 0 & 0 & 0 & 1 \\ 0 & 0 & 1 & 0 \end{bmatrix}}_{CNOT} \cdot \underbrace{\begin{bmatrix} 0 \\ 0 \\ 0 \\ 1 \end{bmatrix}}_{\psi} = \begin{bmatrix} 0+0+0+0 \\ 0+0+0+0 \\ 0+0+0+1 \\ 0+0+0+0 \end{bmatrix} = \begin{bmatrix} 0 \\ 0 \\ 1 \\ 0 \end{bmatrix} \equiv |10\rangle.$$

Quantum circuits are used as proper description for a sequence of quantum operations. A *quantum circuit* [12] consists of a set of qubits, which are vertically aligned in a circuit diagram. The time axis is represented by a horizontal line for each qubit and read from left to right. Boxes on the time axis of a qubit indicate which quantum operation has to be

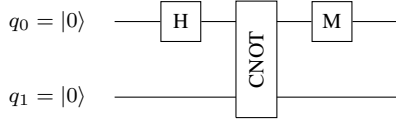


Fig. 1: Quantum circuit

applied. Note that measurement as reviewed in Section II-A and illustrated in Example 1 also counts as quantum operation in this context.

Example 3: Consider the quantum circuit shown in Fig. 1. The circuit contains two qubits, q_0 and q_1 , which are both initialized with basis state $|0\rangle$. Consequently, the initial state is $|\psi\rangle = |00\rangle$. First, a Hadamard operation is applied to qubit q_0 , which is represented by a box labeled H . Then, a $CNOT$ operation, involving both qubits, is performed. Finally, qubit q_0 is measured (represented by a box labeled M), which collapses its superposition into one of the two basis states.

III. CONDUCTING SIMULATION

The basics reviewed in the previous section are sufficient to simulate the execution of quantum operations. In fact, for a given sequence of quantum operations to be simulated, corresponding simulators simply have to conduct the multiplications of each operation matrix U with the respective intermediate quantum states $|\psi\rangle$ as reviewed in Def. 2 and illustrated in Example 2. However, for actual quantum algorithms severe challenges emerge which significantly restrict today's capabilities to simulate quantum computations. In the following, these challenges are discussed – followed by a summary of how state of the art solutions currently deal with them.

A. Exponential Growth

A quantum circuit can be simulated by multiplying all matrices describing the quantum operation (from left to right) successively to the state vector. Therefore, all matrices have to be of dimension $2^n \times 2^n$. Since most quantum operations work on $k < n$ qubits only, their matrices have to be expanded to match the size of the state vector. To this end, an operation matrix for the remaining $n - k$ qubits is required. Since they shall not be affected by the gate, a 2×2 identity matrix I_2 is used for this purpose. The overall $2^n \times 2^n$ -matrix is eventually obtained by forming the Kronecker product of all these matrices.

Example 4: Consider again the quantum circuit shown in Fig. 1 with state $|q_0 q_1\rangle = |00\rangle$ as input. The first operation of the circuit is a Hadamard operation, which is applied to qubit q_0 . Since this operation shall not affect q_1 , we form the Kronecker product of H and the identity matrix I_2

$$H \otimes I_2 = \frac{1}{\sqrt{2}} \begin{bmatrix} 1 & 1 \\ 1 & -1 \end{bmatrix} \otimes \begin{bmatrix} 1 & 0 \\ 0 & 1 \end{bmatrix} = \frac{1}{\sqrt{2}} \begin{bmatrix} 1 & 0 & 1 & 0 \\ 0 & 1 & 0 & 1 \\ 1 & 0 & -1 & 0 \\ 0 & 1 & 0 & -1 \end{bmatrix}.$$

Multiplying this matrix with the state vector yields

$$\psi' = \frac{1}{\sqrt{2}} \begin{bmatrix} 1 & 0 & 1 & 0 \\ 0 & 1 & 0 & 1 \\ 1 & 0 & -1 & 0 \\ 0 & 1 & 0 & -1 \end{bmatrix} \cdot \begin{bmatrix} 1 \\ 0 \\ 0 \\ 0 \end{bmatrix} = \frac{1}{\sqrt{2}} \begin{bmatrix} 1 \\ 0 \\ 1 \\ 0 \end{bmatrix}.$$

Applying the $CNOT$ operation yields

$$\psi'' = \begin{bmatrix} 1 & 0 & 0 & 0 \\ 0 & 1 & 0 & 0 \\ 0 & 0 & 0 & 1 \\ 0 & 0 & 1 & 0 \end{bmatrix} \cdot \frac{1}{\sqrt{2}} \begin{bmatrix} 1 \\ 0 \\ 1 \\ 0 \end{bmatrix} = \frac{1}{\sqrt{2}} \begin{bmatrix} 1 \\ 0 \\ 0 \\ 1 \end{bmatrix}.$$

Since both, the state vectors as well as the operation matrices grow exponentially with respect to the number n of qubits, a crucial obstacle becomes evident: The simulation of quantum computations requires an exponential amount of space. The same complexity applies for the measurement of a quantum state, since, because of superposition, also the state vector may contain an exponentially large number of non-zero entries.

Now, one might think that a local consideration of qubits during the simulation avoids this exponential blow-up: Instead of forming a $2^n \times 2^n$ -matrix using the Kronecker product, a simple application of an operation matrix to only those qubits which are actually affected might be sufficient. Unfortunately, this is not possible, since *entanglement*, which is one of the main concepts that make quantum computations superior to classical computations, frequently occurs [12]. Two qubits are entangled if their state cannot be described without the other. An example illustrates the concept:

Example 4 (continued): Consider again the quantum state $|\psi''\rangle$ from above. If we e.g. measure q_0 , this qubit collapses to the basis state $|0\rangle$ or $|1\rangle$ with a probability $\left|\frac{1}{\sqrt{2}}\right|^2 = \frac{1}{2}$. But due to the nature of $|\psi''\rangle$, this measurement also affects q_1 . More precisely, if the measurement yields e.g. the basis state $|0\rangle$ for q_0 , the new state vector is $\psi' = [1, 0, 0, 0]^T$, i.e. also q_1 collapses to the basis state $|0\rangle$ (although not explicitly measured). This happens because $|\psi''\rangle$ represents a state in which both qubits are entangled.

Since actual quantum computations frequently use entangled states, a local consideration of qubits affected by an operation is often not possible. Instead the complete (exponential) state vector is required.

B. State-of-the-Art Solutions

In the recent past, researchers and engineers intensely considered this problem and developed corresponding solutions for the simulation of quantum computations. This led to the following state of the art approaches available today:

- *Quipper* [5]: A programming language designed to control future quantum computers. With the language comes

a quantum simulator which conducts the respective operations in a rather straight-forward fashion (i.e. with an exponential representation of vectors and matrices).

- *LIQUI* [21]: Microsoft's tool suite for quantum computation with an integrated quantum simulator which also relies on a straight-forward representation and, thus, also can simulate systems with up to approximately 30 qubits only, when used on a Desktop machine with 32 GB RAM (still requires substantial run-times of up to several days).
- *qHiPSTER* [18]: A quantum high performance software testing environment developed in Intel's Parallel Computing Lab. Here, parallel algorithms are utilized which are executed on 1000 compute nodes with 32 TB RAM distributed across these nodes. Even with this massive hardware power, quantum systems of rather limited size (not more than 40 qubits) can be simulated.
- *Quantum Emulator proposed in* [7]: A solution which utilizes a higher level description of quantum computations (e.g. addition, quantum Fourier transformation, etc.) to directly compute intermediate results instead of applying the individual quantum operations successively. Experimental results are provided for systems with up to 36 qubits which, again, were accomplished with massive hardware power, i.e. a supercomputer similar to the one used for *qHiPSTER*.
- *QX* [9]: A high-performance quantum computer simulation platform developed in the QuTech Computer Engineering Lab at Delft University. The simulator tries to parallelize the application of quantum gates to improve the performance. The authors state that *QX* allows for simulation of 34 fully entangled qubits on a single node using 270 GB of memory.

Overall, all solutions which have been proposed thus far are rather limited, since they rely on a straight-forward representation of quantum states and operations (besides minor optimization, mainly representations such as simple 1-dimensional and 2-dimensional arrays are employed). Consequently, only experimental results for quantum systems with up to 34 qubits were reported on Desktop machines. In order to simulate quantum systems composed of more qubits, solutions exploiting massive hardware power (supercomputers composed of thousands of nodes and more than a petabyte of distributed memory) are applied. But even then, quantum systems with 46 qubits are today's practical limit [18].

IV. GENERAL IDEA

In this work, we propose a complementary simulation approach which *explicitly addresses* the exponential complexity rather than aims to tackle it with massive hardware power. Instead of taking a straight-forward approach for the representation and manipulation of the respective quantum states and operations, we use decision diagrams to exploit redundancies – leading to a significantly more compact representation.

Decision diagrams have already been utilized to represent quantum operations, e.g. in terms of *Quantum Information Decision Diagrams* (QuIDDs [19]) or *Quantum Multiple-Valued Decision Diagrams* (QMDDs [15]). However, they did not get established yet for the purposes of simulation of complex quantum computations. In fact, QuIDDs and QMDDs have been applied to efficiently solve design tasks such as verification and synthesis (see e.g. [22], [14], [13]), while, with respect to simulation, approaches based on decision diagrams have been considered thus far for rather few and small quantum computations only [20].

In the following, we aim for closing the gap between a compact representation and efficient simulation of quantum computations. To this end, we develop a compact representation for state vectors which, afterwards, is extended by a second dimension – leading to a compact representation of quantum operations. Finally, we show how simulation can efficiently be conducted on the resulting representations. This includes multiplication of a state vector and a matrix as well as measurement of individual qubits.

A. Representation of State Vectors

As discussed in Section II-A, a system composed of n qubits is represented with a state vector of size 2^n – an exponential representation. However, a closer look at state vectors unveils that they are frequently composed of redundant entries which provide ground for a more compact representation.

Example 5: Consider a quantum system with $n = 3$ qubits situated in a state given by the following vector:

$$\psi = \left[0, 0, \frac{1}{2}, 0, \frac{1}{2}, 0, -\frac{1}{\sqrt{2}}, 0 \right]^T.$$

Although of exponential size ($2^3 = 8$ entries), this vector only assumes three different values, namely 0, $\frac{1}{2}$, and $-\frac{1}{\sqrt{2}}$.

This redundancy can be exploited for a more compact representation. To this end, decision diagram techniques are employed. For classical computations, e.g. *Binary Decision Diagrams* (BDDs, [3]) are very well known. Here, a decomposition scheme is employed which reduces a function to be represented into corresponding sub-functions. Since they also usually include redundancies, equivalent sub-functions result which can be shared – eventually yielding a much more compact representation. In a similar fashion, the concept of decomposition can also be applied to represent state vectors in a more compact fashion.

More precisely, similar to decomposing a function into sub-functions, we decompose a given state vector with its complex entries into sub-vectors. To this end, consider a quantum system with qubits q_0, q_1, \dots, q_{n-1} , whereby q_0 represents the most significant qubit. Then, the first 2^{n-1} entries of the corresponding state vector represent the amplitudes for the basis states with q_0 set to $|0\rangle$; the other entries represent the

amplitudes for states with q_0 set to $|1\rangle$. This decomposition is represented in a decision diagram structure by a node labeled q_0 and two successors leading to nodes representing the sub-vectors. The sub-vectors are recursively decomposed further until vectors of size 1 (i.e. a complex number) results. This eventually represents the amplitude α_i for the complete basis state and is given by a terminal node. During these decompositions, equivalent sub-vectors can be represented by the same nodes – allowing for sharing and, hence a reduction of the complexity of the representation. An example illustrates the idea.

Example 6: Consider again the quantum state from Example 5. Applying the decompositions described above yields a decision diagram as shown in Fig. 2a. The left (right) outgoing edge of each node labeled q_i points to a node representing the sub-vector with all amplitudes for the basis states with q_i set to $|0\rangle$ ($|1\rangle$). Following a path from the root to the terminal yields the respective entry. For example, following the path highlighted bold in Fig. 2a provides the amplitude for the basis state with $q_0 = |1\rangle$ (right edge), $q_1 = |1\rangle$ (right edge), and $q_2 = |0\rangle$ (left edge), i.e. $-\frac{1}{\sqrt{2}}$ which is exactly the amplitude for basis state $|110\rangle$ (seventh entry in the vector from Example 5). Since some sub-vectors are equal (e.g. $[\frac{1}{2}, 0]^T$ represented by the left node labeled q_2) sharing is possible.

However, even more sharing is possible. In fact, many entries of the state vectors differ in a common factor only (e.g. the state vector from Example 5 has entries $\frac{1}{2}$ and $-\frac{1}{\sqrt{2}}$ which differ by the factor $-\sqrt{2}$ only). This is additionally exploited in the proposed representation by denoting common factors of amplitudes as weights to the edges of the decision diagram. Then, the value of an amplitude for a basis state is determined by not only following the path from the root to the terminal, but additionally multiplying the weights of the edges along this path. Again, an example illustrates the idea.

Example 7:

Consider again the quantum state from Example 5 and the corresponding decision diagram shown in Fig. 2a. As can be seen, the sub-trees rooting the node labeled q_2 are structurally equivalent and only differ in their terminal values. Moreover, they represent sub-vectors $[\frac{1}{2}, 0]^T$ and $[-\frac{1}{\sqrt{2}}, 0]^T$ which only differ in a common factor.

In the decision diagram shown in Fig 2b, both sub-trees are merged. This is possible since the corresponding value of the amplitudes is now determined not by the terminals, but the weights on the respective paths. As an example, consider again the path highlighted bold representing the amplitude for the basis state $|110\rangle$. Since this path includes the weights $\frac{1}{2}$, 1, $-\sqrt{2}$, and 1, an amplitude value of $\frac{1}{2} \cdot 1 \cdot (-\sqrt{2}) \cdot 1 = -\frac{1}{\sqrt{2}}$ results.

Note that, of course, various possibilities exist to factorize an amplitude. Hence, we apply a normalization which assumes

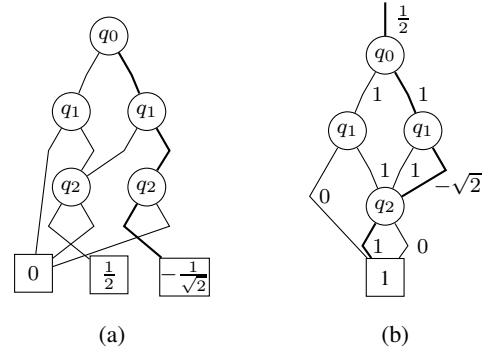


Fig. 2: Representation of the state vector

the left edge to inherit a weight of 1. More precisely, the weights w_l and w_r of the left and right edge are both divided by w_l and this common factor is propagated upwards to the parents of the node. If $w_l = 0$, the node is normalized by propagating w_r upwards to the parents of the node.¹

B. Representation of Matrices

As discussed in Section II-B, quantum operations are described by unitary matrices. Similar to state vectors, these matrices include redundancies, which can be represented in a more compact fashion. To this end, we extend the proposed decomposition scheme for state vectors by a second dimension – yielding a decomposition scheme for $2^n \times 2^n$ matrices.

The entries of a unitary matrix $U = [u_{i,j}]$ indicate how much the operation U affects the mapping from a basis state $|i\rangle$ to a basis state $|j\rangle$. Considering again a quantum system with qubits q_0, q_1, \dots, q_{n-1} , whereby w.l.o.g. q_0 represents the most significant qubit, the matrix U is decomposed into four sub-matrices with dimension $2^{n-1} \times 2^{n-1}$: All entries in the left upper sub-matrix (right lower sub-matrix) provide the values describing the mapping from basis states $|i\rangle$ to $|j\rangle$ with both assuming $q_0 = |0\rangle$ ($q_0 = |1\rangle$). All entries in the right upper sub-matrix (left lower sub-matrix) provide the values describing the mapping from basis states $|i\rangle$ with $q_0 = |1\rangle$ to $|j\rangle$ with $q_0 = |0\rangle$ ($q_0 = |0\rangle$ to $q_0 = |1\rangle$). This decomposition is represented in a decision diagram structure by a node labeled q_0 and four successors leading to nodes representing the sub-matrices. The sub-matrices are recursively decomposed further until a 1×1 matrix (i.e. a complex number) results. This eventually represents the value $u_{i,j}$ for the corresponding mapping. Also during these decompositions, equivalent sub-matrices are represented by the same nodes and weights as well as a corresponding normalization scheme (as applied for the representation of state vectors) is employed. Note that for a simpler graphical notation, we use zero stubs

¹Applying a fixed normalization scheme, a representation which is even canonic (w.r.t qubit order) results. However, since canonicity is not further relevant for the purpose of simulation, this issue is not discussed in detail in this work.

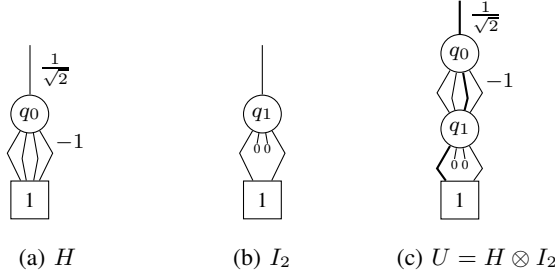


Fig. 3: Representation of matrices

to indicate zero matrices (i.e. matrices that contain zeros only) and omit edge weights that are equal to one. Again, an example illustrates the idea.

Example 8: Consider again the matrices of H , I_2 , and $U = H \otimes I_2$ from Example 4. Fig. 3 shows the corresponding decision diagram representations. The Kronecker product $U = H \otimes I_2$ was efficiently constructed by taking the decision diagram representation of H and replacing its terminal node with the root node of the decision diagram representing I_2 . Following the path highlighted bold in Fig. 3c defines the entry $u_{0,2}$: a mapping from $|0\rangle$ to $|1\rangle$ for q_0 (third edge from the left) and from $|0\rangle$ to $|0\rangle$ for q_1 (first edge). Consequently the path describes the entry for a mapping from $|00\rangle$ to $|10\rangle$. Multiplying all factors on the path yields $\frac{1}{\sqrt{2}} \cdot 1 \cdot 1 = \frac{1}{\sqrt{2}}$, which is the value of $u_{0,2}$.

C. Multiplying Unitary Matrices

With the availability of a compact representation of state vectors and unitary matrices, it is left to provide corresponding methods for conducting quantum operations, i.e. multiplication of vectors with matrices as well as measurement. Also here, a decompositional scheme can be applied. The vector/matrix-multiplication as defined in Def. 2 can also be decomposed with respect to the most significant qubit leading to

$$\psi'_i = \sum_{k=0}^{2^n-1} u_{i,k} \cdot \psi_k = \sum_{k=0}^{2^{n-1}-1} u_{i,k} \cdot \psi_k + \sum_{k=2^{n-1}}^{2^n-1} u_{i,k} \cdot \psi_k,$$

or, using the matrix notation,

$$U \cdot \psi = \begin{bmatrix} U_{00} & U_{10} \\ U_{10} & U_{11} \end{bmatrix} \cdot \begin{bmatrix} \psi_0 \\ \psi_1 \end{bmatrix} = \begin{bmatrix} U_{00} \cdot \psi_0 \\ U_{10} \cdot \psi_0 \end{bmatrix} + \begin{bmatrix} U_{01} \cdot \psi_1 \\ U_{11} \cdot \psi_1 \end{bmatrix}.$$

This means, that we have to recursively determine² the four sub-products $U_{00} \cdot \psi_0$, $U_{01} \cdot \psi_1$, $U_{10} \cdot \psi_0$, and $U_{11} \cdot \psi_1$. As shown in Fig. 4, these sub-products are then combined with a decision diagram node to two intermediate state vectors. Finally, these

²The decompositions of multiplication and addition are recursively applied until 1×1 matrices or 1-dimensional vectors result. Since those eventually represent just complex numbers, their multiplication and/or addition is straight-forward.

intermediate state vectors have to be added. This addition can be recursively decomposed in a similar fashion.

$$\psi + \phi = \begin{bmatrix} \psi_0 \\ \psi_1 \end{bmatrix} + \begin{bmatrix} \phi_0 \\ \phi_1 \end{bmatrix} = \begin{bmatrix} \psi_0 + \phi_0 \\ \psi_1 + \phi_1 \end{bmatrix}.$$

The recursively determined sub-sums $\psi_0 + \phi_0$ and $\psi_1 + \phi_1$ are composed by a decision diagram node as shown in Fig. 5.

Moreover, all these decompositions into sub-products and sub-sums do not change the decision diagram structure. Hence, the complexity of them remains bounded by the number of nodes of the original representations. Furthermore, redundancies can again be exploited by chaching sub-products and sub-sums.

D. Measurement

Measurement can also efficiently be performed on the decision diagram structure. To this end, consider w.l.o.g. that qubit q_0 (which is represented by the root node of the corresponding decision diagram) of the state vector should be measured (this can easily be accomplished by re-arranging the nodes and edges of the decision diagram). Then, the left (right) successor of the root node represents the sub-vector containing the amplitudes of all states with $q_0 = |0\rangle$ ($q_0 = |1\rangle$), i.e. states that are of form $|0q_1q_2\dots\rangle$ ($|1q_1q_2\dots\rangle$). The probability for collapsing qubit q_0 to state $|0\rangle$ (state $|1\rangle$) is the sum of the squared magnitudes of the complex entries in the corresponding sub-vector, i.e.

$$P(q_0 \rightarrow |0\rangle) = \sum_{x \in \{0,1\}^{n-1}} |\alpha_x|^2$$

$$P(q_0 \rightarrow |1\rangle) = \sum_{x \in \{0,1\}^{n-1}} |\alpha_x|^2.$$

Example 9: Consider again the quantum state discussed in Example 5. The probabilities for measuring $q_0 = |0\rangle$ and $q_0 = |1\rangle$ are:

$$P(q_0 \rightarrow |0\rangle) = |0|^2 + |0|^2 + \left|\frac{1}{2}\right|^2 + |0|^2 = \frac{1}{4}$$

$$P(q_0 \rightarrow |1\rangle) = \left|\frac{1}{2}\right|^2 + |0|^2 + \left|-\frac{1}{\sqrt{2}}\right|^2 + |0|^2 = \frac{3}{4}$$

Therefore, the qubit q_0 is collapsed into basis state $|0\rangle$ (basis state $|1\rangle$) with a probability of 0.25 (0.75).

To this end, we have to determine the summed probabilities for the decision diagram nodes. Again, the calculation of these probabilities can recursively be decomposed since

$$\sum_{x \in \{0,1\}^{n-1}} |\alpha_x|^2 = \sum_{x \in 00\{0,1\}^{n-2}} |\alpha_x|^2 + \sum_{x \in 01\{0,1\}^{n-2}} |\alpha_x|^2.$$

This means we have to recursively determine the summed probabilities p_{left} and p_{right} of the sub-vectors. As Fig. 6 shows, the summed probability of the current decision diagram

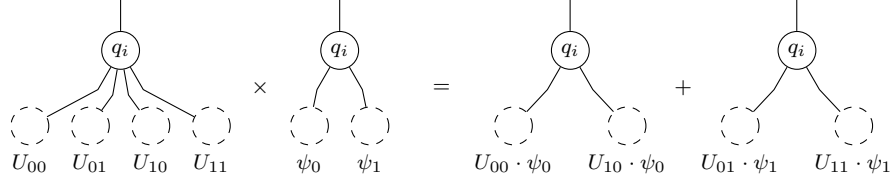


Fig. 4: Multiplication of a unitary matrix and a state-vector

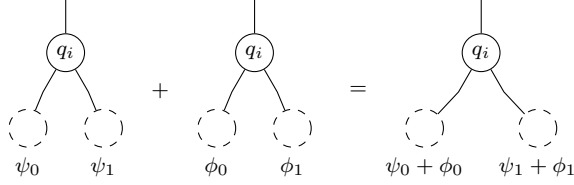


Fig. 5: Addition of state-vectors

$$p = p_{left} \cdot w_l^2 + p_{right} \cdot w_r^2$$

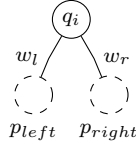


Fig. 6: Probability of a decision diagram node

node is then determined by the sum of the probabilities of the sub-vectors. Before these probabilities are added, they are multiplied with the squared weight of the respective edges.

Note that, in our decision diagram representation, the amplitudes α_x of the 2^n basis states are determined by a product of $n+1$ edge weights, i.e. $\alpha_x = w_{x,0} \cdot w_{x,1} \cdots w_{x,n}$. Also, $|\alpha_x|^2$ can directly be determined on the decision diagram, since

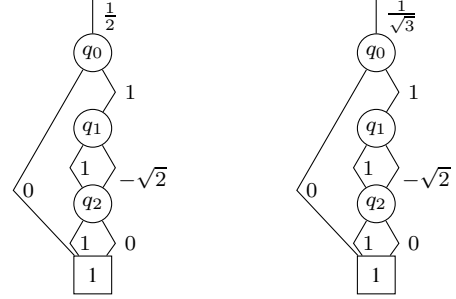
$$|\alpha_x|^2 = |w_{x,0} \cdot w_{x,1} \cdots w_{x,n}|^2 = |w_{x,0}|^2 \cdot |w_{x,1}|^2 \cdots |w_{x,n}|^2.$$

Finally, the weight on the edges to the left and the right successor of the root nodes have to be considered to obtain the correct probabilities $P(q_0 \rightarrow |0\rangle)$ and $P(q_0 \rightarrow |1\rangle)$. An example illustrates the idea.

Example 9: The decision diagram shown in Fig 2b represents the quantum state ψ (cf. Example 5). The probability of the node labeled q_2 can be determined by $1^2 + 0^2 = 1$. Based on that, the probabilities of the two nodes labeled q_1 can be determined. These are $0^2 \cdot 1 + 1^2 \cdot 1 = 1$ for the left node and $1^1 \cdot 1 + |-\sqrt{2}|^2 \cdot 1 = 3$ for the right node. From these nodes, we can determine the probabilities for collapsing q_0 to basis state $|0\rangle$ or $|1\rangle$ by:

$$P(q_0 \rightarrow |0\rangle) = \left(\frac{1}{2}\right)^2 \cdot 1^2 \cdot 1 = \frac{1}{4}$$

$$P(q_0 \rightarrow |1\rangle) = \left(\frac{1}{2}\right)^2 \cdot 1^2 \cdot 3 = \frac{3}{4}$$

(a) Measure $q_0 = |1\rangle$

(b) Normalize amplitudes

Fig. 7: Measurement of qubit q_0

Having the probabilities for collapsing q_0 to basis state $|0\rangle$ and $|1\rangle$ allows to sample the new value for q_0 . If we obtain basis state $|0\rangle$ (basis $|1\rangle$), the amplitudes for all basis states with $q_0 = |1\rangle$ ($q_0 = |0\rangle$) drop to zero. In the decision diagram, we perform this collapse by changing the right (left) outgoing edge of the root node to point to the terminal and attach weight zero. Finally, the remaining (non-zero) amplitudes in the state vector must be modified in order to fulfill the normalization constraint (cf. Section II-A). To this end, all amplitudes are divided by $\sqrt{P(q_0 \rightarrow |0\rangle)}$ ($\sqrt{P(q_0 \rightarrow |1\rangle)}$). This can easily be conducted on the decision diagram structure by modifying the weight of the edge to the root node.

Example 9 (continued): Assume we measure basis state $|1\rangle$ for qubit q_0 . Fig. 7a shows the resulting decision diagram. To fulfill the normalization constraint, we divide the weight of the edge to the root node by $\sqrt{\frac{3}{4}}$ – eventually resulting in the decision diagram shown in Fig. 7b.

V. EXPERIMENTAL RESULTS

We evaluated the scalability of the proposed approach and compare it to the state-of-the-art. To this end, we implemented the simulator in C++³ on top of the QMDD package provided by [15], which we extended and modified to realize the concepts introduced above. As state-of-the-art we considered the publicly available implementations of the recently proposed simulators *LIQUi|* [21] and *QX* [9]. All simulations have been conducted on a regular Desktop computer, i.e. a 64-bit machine with 4 cores (8 threads) running at a clock frequency

³The implementation is publicly available at http://www.jku.at/iic/eda/quantum_simulation

of 3.8 GHz and 32 GB of memory running Linux 4.4⁴. Besides that, we additionally considered the best results published for other simulators (cf. Section III-B) that have been taken from the respective papers.

As benchmarks, well-known quantum algorithms considered by previous work have been used. More precisely, quantum systems generating entangled states, conducting *Quantum Fourier Transformation* (QFT; cf. [12]), executing Grover's Algorithm for database search [6], and executing Shor's Factorization Algorithm [17] (using the realization proposed by Beauregard [2] that requires $2n + 3$ qubits to factor an n -bit integer) have been considered. Note that, for all benchmarks except QFT, the initial assignments of the inputs are fixed. For the Quantum Fourier Transformation, we randomly chose one of the basis states as initial input assignment.

In order to not run into numerical issues when normalizing the decision diagrams (which requires many divisions), we used the *GNU MPFR* library [1] to increase the precision of the floating point numbers and checked at each measurement whether the probabilities for measuring one of the basis states sum up to one (except a tiny ϵ). In fact, using a precision of 200 bits was enough to avoid numerical errors for all considered benchmarks.

Table I summarizes the results. The columns *#Qubits* and *#Ops* list the number of involved qubits and the number of quantum operations to be conducted, respectively. Columns four and five list the simulation time (in CPU seconds) when using LIQUI| and QX, respectively. The next two columns list the simulation time of the proposed approach as well as the maximal number of nodes required for the representation of the intermediate states and operations. Besides that, Table I also provides a comparison to other state-of-the-art simulation approaches. That is, whenever results from them are provided in the literature, the respectively best result for a considered quantum algorithm is summarized in the rightmost column.

Note that, in the publicly available version of LIQUI|, circuits composed of at most 23 qubits can be simulated. Using QX, we were able to simulate up to 30 qubits on our machine – trying to allocate 31 or more qubits failed (due to limited memory). Furthermore, QX does not allow to simulate Beauregard's realization of Shor's algorithm for integer factorization, because of missing features in the circuit description language (since QX is still in its infancy). We have accordingly marked all these cases by *n.a.* (not applicable) in Table I.

As can be seen, the simulation of quantum systems generating entangled states and conducting QFT shows a linear behavior on our simulator. While this allows for a rather unlimited scalability using the solution proposed in this work,

Microsoft's simulator LIQUI| [21] as well as QX show exponential behavior. Even massive hardware power such as employed by Intel's simulator *qHIPSTER* [18] (running on a machine with 1000 nodes and 32 terabytes of memory) or the quantum emulator of [7] (running on a similar machine) manages to conduct QFT for a maximum of 40 qubits only (and additionally requires hundreds of seconds, while the approach proposed in this work terminates in a fraction of a second).

The simulation of Grover's Algorithm and Shor's Algorithm constitutes a more challenging task. But even here, the proposed representation remains rather compact. For example, in case of simulating Shor's Algorithm with 37 qubits, only slightly more than 50 000 nodes are required.⁵ In fact, the significantly larger number of operations is more challenging here. Nevertheless, the proposed approach still manages to simulate both algorithms significantly more efficient and for more qubits than the state-of-the-art. While Microsoft's simulator LIQUI| is capable of conducting Shor's Algorithm for at most 31 qubits in more than 30 days (on a similar machine; cf. [21]), the simulation approach proposed in this work completes this task within a bit more than a minute.

Overall, the proposed simulation approach clearly outperforms the current state-of-the-art in terms of runtime and, additionally, is able to simulate quantum computations with more qubits. Besides that, all these accomplishments can be achieved on a single core of a regular Desktop machine, i.e. without massive hardware power – leading to a substantial increase of scalability.

VI. CONCLUSION

This work introduces a complementary new approach for the simulation of quantum computations. Instead of relying on massive hardware power (as done by the state-of-the-art and still proposed in recent roadmaps such as discussed in [18]), the solution presented in this work proposes an alternative direction based on a more compact representation. To this end, we revisited the basics of quantum computation and developed a simulation approach which exploits redundancies in the respective quantum state and operation descriptions. The resulting simulator (which is publicly available at http://www.jku.at/iic/eda/quantum_simulation) is capable of (1) simulating quantum computations with more qubits than before, (2) in significantly less run-time (in hours or, in many cases, just minutes or seconds rather than several days), and that (3) on a regular Desktop machine (rather than supercomputers).

⁴The proposed approach currently uses a single core while the simulators LIQUI| and QX use multiple threads.

⁵Note that the number of required decision diagram nodes is directly proportional to the memory consumption, which is therefore magnitudes lower than compared to the state-of-the-art.

TABLE I: Experimental results

Computation	#Qubits	#Ops	LIQUi ⟩ [21] Time [s]	QX [9] Time [s]	Proposed approach Time [s] #Nodes	Best results reported for the state-of-the-art
Entanglement	22	22	0.60	0.37	<0.01 43	• QX [9]: max. 34 qubits using less than 270 GB of memory
	23	23	1.26	0.80	<0.01 45	
	24	24	n.a.	1.67	<0.01 47	
	26	26	n.a.	6.49	<0.01 51	
	28	28	n.a.	29.99	<0.01 55	
	30	30	n.a.	255.80	<0.01 59	
	100	100	n.a.	n.a.	<0.01 199	
QFT	22	253	9.28	6.85	0.01 22	• qHiPSTER (Intel, cf. [18]): max. 40 qubits on a supercomputer (in approx. 1000 s). • Quantum emulator from [7]: max. 36 qubits on a supercomputer (in approx. 10 s).
	23	276	20.96	14.59	0.01 23	
	24	300	n.a.	34.38	0.01 24	
	26	351	n.a.	139.34	0.02 26	
	28	406	n.a.	594.42	0.02 28	
	30	465	n.a.	9485.09	0.02 30	
Grover	100	5050	n.a.	n.a.	0.36 100	
	14	5054	11.82	6.31	0.23 53	
	16	11 600	99.86	55.70	0.70 61	
	18	26 082	879.53	578.14	1.74 69	
	20	57 940	8828.54	6303.97	3.78 77	
	21	86 037	>18 000	>18 000	8.85 81	
	30	2 780 430	n.a.	>18 000	208.265 256	
Shor	40	118 632 840	n.a.	n.a.	2 599.14 346	• LIQUi ⟩ (Microsoft, cf. [21]): max. 31 qubits (in more than 30 days).
	19	61510	195.911	n.a.	5.87 296	
	21	92 700	1038.49	n.a.	7.83 215	
	23	134 490	5098.41	n.a.	16.51 349	
	31	451 577	n.a.	n.a.	75.72 305	
	33	581 272	n.a.	n.a.	1 262.37 6 508	
	35	737 214	n.a.	n.a.	3 061.68 8 933	
	37	922 385	n.a.	n.a.	16 919.70 51 195	

REFERENCES

- [1] The GNU MPFR library. <http://www.mpfpr.org>.
- [2] S. Beauregard. Circuit for Shor's algorithm using $2n+3$ qubits. *Quantum Information & Computation*, 3(2):175–185, 2003.
- [3] R. E. Bryant. Graph-based algorithms for Boolean function manipulation. *IEEE Transactions on Computers*, 35(8):677–691, 1986.
- [4] S. Debnath, N. Linke, C. Figgatt, K. Landsman, K. Wright, and C. Monroe. Demonstration of a small programmable quantum computer with atomic qubits. *Nature*, 536(7614):63–66, 2016.
- [5] A. S. Green, P. L. Lumsdaine, N. J. Ross, P. Selinger, and B. Valiron. Quipper: a scalable quantum programming language. In *Conference on Programming Language Design and Implementation*, pages 333–342, 2013.
- [6] L. K. Grover. A fast quantum mechanical algorithm for database search. In *Symposium on the Theory of Computing*, pages 212–219, 1996.
- [7] T. Häner, D. S. Steiger, M. Smelyanskiy, and M. Troyer. High performance emulation of quantum circuits. In *International Conference for High Performance Computing, Networking, Storage and Analysis*, page 74, 2016.
- [8] D. Hanneke, J. Home, J. Jost, J. Amini, D. Leibfried, and D. Wineland. Realization of a programmable two-qubit quantum processor. *Nature Physics*, 6(1):13–16, 2010.
- [9] N. Khammassi, I. Ashraf, X. Fu, C. Almudever, and K. Bertels. QX: A high-performance quantum computer simulation platform. In *Design, Automation and Test in Europe*, 2017.
- [10] N. M. Linke, D. Maslov, M. Roetteler, S. Debnath, C. Figgatt, K. A. Landsman, K. Wright, and C. Monroe. Experimental comparison of two quantum computing architectures. *Proceedings of the National Academy of Sciences*, page 201618020, 2017.
- [11] T. Monz, D. Nigg, E. A. Martinez, M. F. Brandl, P. Schindler, R. Rines, S. X. Wang, I. L. Chuang, and R. Blatt. Realization of a scalable shor algorithm. *Science*, 351(6277):1068–1070, 2016.
- [12] M. Nielsen and I. Chuang. *Quantum Computation and Quantum Information*. Cambridge Univ. Press, 2000.
- [13] P. Niemann, R. Datta, and R. Wille. Logic synthesis for quantum state generation. In *Multiple-Valued Logic (ISMVL), 2016 IEEE 46th International Symposium on*, pages 247–252. IEEE, 2016.
- [14] P. Niemann, R. Wille, and R. Drechsler. Efficient synthesis of quantum circuits implementing Clifford group operations. In *Asia and South Pacific Design Automation Conference*, pages 483–488, 2014.
- [15] P. Niemann, R. Wille, D. M. Miller, M. A. Thornton, and R. Drechsler. QMDDs: Efficient quantum function representation and manipulation. *IEEE Transactions on CAD*, 35(1):86–99, 2016.
- [16] M. Reed, L. DiCarlo, S. Nigg, L. Sun, L. Frunzio, S. Girvin, and R. Schoelkopf. Realization of three-qubit quantum error correction with superconducting circuits. *Nature*, 482(7385):382–385, 2012.
- [17] P. W. Shor. Polynomial-time algorithms for prime factorization and discrete logarithms on a quantum computer. *SIAM Journal on Computing*, 26(5):1484–1509, 1997.
- [18] M. Smelyanskiy, N. P. D. Sawaya, and A. Aspuru-Guzik. qHiPSTER: The quantum high performance software testing environment. *CoRR*, abs/1601.07195, 2016.
- [19] G. F. Viamontes, I. L. Markov, and J. P. Hayes. Improving gate-level simulation of quantum circuits. *Quantum Information Processing*, 2(5):347–380, 2003.
- [20] G. F. Viamontes, I. L. Markov, and J. P. Hayes. *Quantum Circuit Simulation*. Springer, 2009.
- [21] D. Wecker and K. M. Svore. LIQUi|⟩: A software design architecture and domain-specific language for quantum computing. *CoRR*, abs/1402.4467, 2014.
- [22] R. Wille, D. Große, D. M. Miller, and R. Drechsler. Equivalence checking of reversible circuits. In *International Symposium on Multi-Valued Logic*, pages 324–330, 2009.